### Performance Optimization of a Superheated Steam Rankine Cycle for a Molten Salt Reactor

Doh Hyeon Kim<sup>a</sup>, Jeong Ik Lee<sup>a\*</sup>

<sup>a</sup> Department of Nuclear and Quantum Engineering, Korea Advanced Institute of Science and Technology (KAIST)

\*Corresponding author: jeongiklee@kaist.ac.kr

\*Keywords: Molten Salt Reactor (MSR), Steam Rankine Cycle, Steam Generator, Solidification

#### 1. Introduction

The growing global demand for energy, coupled with the urgent need to address climate change, underscores the importance of developing the next-generation nuclear systems. Among these, the Generation IV reactors are being actively researched with the goals of enhanced safety, sustainability, economic competitiveness, and resistance to nuclear proliferation. In particular, molten salt reactors (MSRs) have attracted significant attention as a promising design due to their high thermal efficiency and inherent safety features [1][2].

MSRs operate at near-atmospheric pressure, inherently reducing the likelihood of high-pressure accidents, and produce high-temperature heatexceeding 550 °C—that enables superior thermal efficiency. In addition, the potential for online fuel reprocessing reduces nuclear waste generation and allows the use of alternative fuels such as thorium, further enhancing their sustainability [2][3]. To realize these advantages on a commercial scale, the design optimization of the power conversion systemresponsible for transforming high-temperature nuclear heat into electricity—must be addressed as a critical prerequisite. Candidate power cycles compatible with MSRs include the superheated steam Rankine cycle, the supercritical steam Rankine cycle, and the supercritical CO<sub>2</sub> (sCO<sub>2</sub>) Brayton cycle [4][5]. Among these, the superheated steam Rankine cycle currently offers the highest technology maturity and reliability, making it the most commercially viable option in the near term [6].

The high operating temperature of MSRs provides ideal conditions for maximizing the efficiency of the conventional and well-established steam Rankine cycle. The thermal efficiency of the Rankine cycle is primarily determined by the inlet temperature and pressure of the steam supplied to the turbine [7]. Thus, fully utilizing the high-temperature output of the MSR to achieve highpressure, high-temperature steam is a decisive factor in the overall plant economics. Modern large-scale power plants employ regenerative feedwater heating extracting steam from intermediate turbine stages to preheat the feedwater—to improve efficiency. However, increasing the bleed steam flow benefits feedwater heating but simultaneously reduces the steam flow through the main turbine, potentially lowering the net output [8]. This trade-off motivates the present study,

which analyzes the effects of varying the bleed flow to the feedwater heaters and the extraction flow downstream of the high-pressure turbine on both cycle efficiency and steam generator inlet temperature in an MSR-coupled superheated steam Rankine cycle.

In MSRs, molten salts serve as the primary coolant, and the choice of salt determines the operating temperature range and heat transfer characteristics of the reactor. In particular, the melting point of the molten salt is one of the most critical parameters for defining the thermal boundary conditions at the steam generator—the interface between the reactor and the power conversion system. If the salt temperature in the steam generator drops below its melting point, solidification can occur, blocking flow channels and causing severe operational issues [9][10][11]. Accordingly, in this study, the inhouse power system analysis code KAIST-CCD was employed to optimize the power cycle based on the steam outlet conditions of the steam generator in a molten salt reactor (MSR). The resulting variations in overall cycle efficiency and the steam generator inlet temperature were examined. Furthermore, the steam generator inlet temperature was compared with the melting points of representative fluoride- and chloride-based molten salts under consideration for MSR applications. This comparison allowed us to evaluate the maximum attainable feedwater temperature at the steam generator inlet. These findings provide valuable insights for the future design of steam Rankine cycles tailored for molten salt reactors.

# 2. Rankine Cycle Optimization

Candidates of power conversion systems for MSRs include the superheated steam Rankine cycle, the supercritical steam Rankine cycle, and the sCO2 Brayton cycle. Among these, the superheated steam Rankine cycle is considered the most practical option, as it has already accumulated extensive operational experience and reached a high level of technological maturity, with most components having been commercialized. In fact, additional technical challenges are largely confined to the design of the steam generator that utilizes molten salt as the heat source, while the remaining parts of the cycle can rely on established technologies.

In contrast, the supercritical steam Rankine cycle and the sCO<sub>2</sub> Brayton cycle allow for higher inlet temperatures of the feedwater or sCO<sub>2</sub>, thereby offering the advantage of being less constrained by molten salt solidification issues. However, these cycles have not yet achieved sufficient commercialization and still face limitations due to the lack of extensive demonstration and validation. Therefore, at the current stage, the superheated steam Rankine cycle is regarded as the most promising option for application to MSRs. Nevertheless, its deployment requires a precise assessment of the molten salt solidification margin, which remains a critical research task.

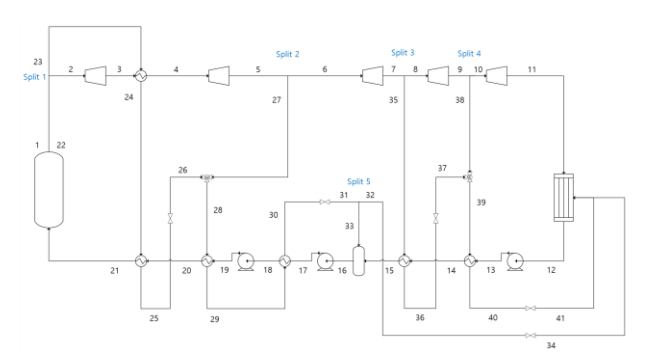


Fig 1. Superheated Steam Rankine Cycle Layout

Accordingly, in this study, the KAIST-CCD code was employed to evaluate the steam generator inlet temperature and overall cycle efficiency for a superheated steam cycle layout, assuming a steam generator outlet temperature of 550°C and outlet pressure of 17.5MPa. The configuration of the superheated steam cycle is presented in Figure 1. The KAIST-CCD code is an in-house tool developed at KAIST, which calculates the overall cycle efficiency as well as the thermodynamic states (temperature and pressure) at the inlet and outlet of each component based on component efficiencies and the specified layout. In this study, variations in 'Split Ratio 1' and 'Split Ratio 2' were analyzed to assess their impact on the overall cycle efficiency and the steam generator inlet temperature. For 'Split Ratio 5', adjustments were made to the bypass line—installed to prevent two-phase flow at the pump inlet due to excessive recirculation flow—by reducing it in 1% increments until the pump inlet quality exceeded -0.2.

Table 1. KAIST-CCD Superheated Steam Rankine

Cycle Input Value

Cycle input value		
Parameter	Value	
Turbine efficiency	85%	
Pump efficiency	80%	
Feedwater heater effectiveness	90%	
HX hot side pressure drop	5%	
HX cold side pressure drop	3%	
Generator efficiency	96%	

Condenser outlet temperature	40 °C
Reactor thermal power	300MWth
SG steam outlet temperature	550 °C
SG feedwater inlet pressure	18 MPa
SG steam outlet pressure	17.5 MPa

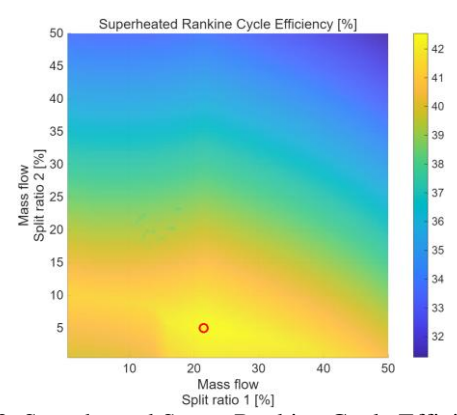


Fig 2. Superheated Steam Rankine Cycle Efficiency

Both Split Ratio 1 and Split Ratio 2 were varied from 0% to 50%, and the resulting cycle efficiencies are presented in Figure 2. The point marked with a red circle represents the case with the highest overall cycle efficiency, which was calculated to be 42.54%. In practice, increasing the split ratio to values approaching 50% introduces significant technical challenges in cycle design and also results in a substantial decrease in cycle efficiency. Therefore, a separate region was defined where the cycle efficiency exceeded 40.0%, and within this region, variations in both the overall cycle efficiency and the steam generator inlet temperature were examined. The cycle efficiency corresponding to this region is shown in Figure 3, while the steam generator inlet temperature is presented in Figure 4.

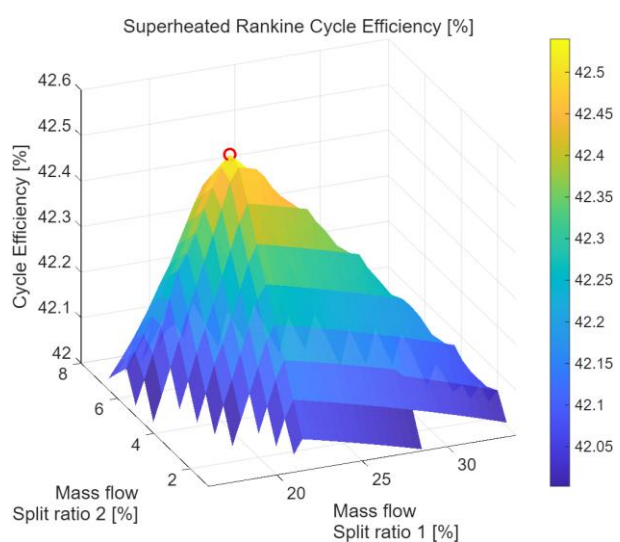


Fig 3. Superheated Steam Rankine Cycle Efficiency (Efficiency > 40% region)

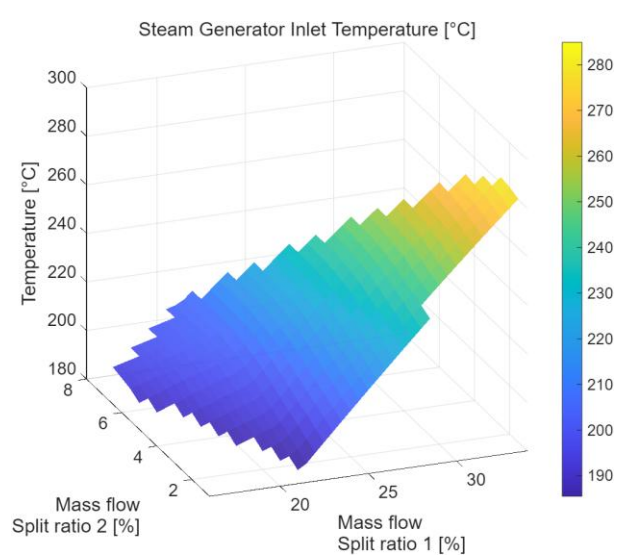


Fig 4. Superheated Steam Rankine Cycle SG Inlet temperature (Efficiency > 40% region)

As expected, an increase in the bypass flow branching from the turbine inlet and passing through the turbine outlet and preheater leads to a rise in the steam generator feedwater temperature. The analysis results similarly confirmed that as the flow fraction branched at the turbine inlet, denoted as "Split Ratio 1," increased, the inlet temperature of the steam generator also increased. Within the region where the cycle efficiency exceeded 40%, the maximum feedwater inlet temperature to the steam generator was found to be 284.9 °C.

#### 3. Candidate Molten Salts for MSR

One of the most distinctive features of modern molten salt reactor (MSR) designs is the adoption of a three-loop heat transport configuration consisting of the primary fuel salt loop, the secondary intermediate heat transfer loop, and the tertiary power conversion system. In particular, the secondary loop serves as a critical safety barrier that physically separates the radioactive primary system from the non-radioactive tertiary power cycle. The choice of coolant for this loop has a profound influence on the overall safety and reliability of the reactor. In theory, the use of low-melting-point nitrateor carbonate-based molten salts—such as Solar Salt—in the secondary loop could be advantageous for preventing coolant freezing and ensuring operational flexibility. However, when the high-temperature operating conditions of MSRs and their unique safety requirements are considered, this approach introduces several major technical challenges that are challenging to resolve.

The most fundamental issue is the thermal instability arising from the low thermal decomposition temperature of such salts. While the primary loop of an MSR typically operates at 600–700 °C, thermal decomposition of nitrate-based Solar Salt begins at approximately 550–

600 °C [12][13]. This means that continuous decomposition could occur in the primary-to-secondary intermediate heat exchanger (IHX), producing noncondensable gases that severely degrade heat transfer performance and necessitate the installation of complex gas management systems.

The second challenge is tritium management [14][15]. Tritium is inevitably generated during MSR operation through fission and neutron capture if the coolant contains lithium (Li). At elevated temperatures, tritium readily permeates metallic structures, allowing it to diffuse into the secondary loop, where it can react with nitrate or carbonate salts to form tritiated water (T2O)—a radiologically hazardous substance that is extremely difficult to separate chemically—thus increasing the burden of radioactive waste management.

Furthermore, accident scenarios involving small leaks in the IHX highlight the hazards of using dissimilar salts. Contact between high-temperature primary salt and low-melting-point secondary salt could cause rapid and violent thermal decomposition, producing large volumes of gas, inducing sudden overpressure in the secondary system, and generating highly corrosive species that accelerate structural degradation.

Considering these combined challenges—thermal stability, radioactive material control, and safety during accident —it is impractical, at the current technological level, to employ low-melting-point nitrate/carbonate salts in the secondary loop of an MSR. The most rational and safe engineering approach is to use chemically compatible and thermally stable molten salts of the same family in both the primary and secondary loops. Specifically, in fast-spectrum MSRs employing the U-Pu fuel cycle, chloride-based molten salts should be used in both loops, while in thermal-spectrum designs using the Th-U fuel cycle, fluoride-based molten salts should be applied consistently in both loops. Accordingly, this study compiles and presents the melting points of fluoride and chloride salts that are considered promising candidates for application in molten salt reactors.

Table 2. Molten salts melting point and maximum working temperature [16][17][18][19]

working temperature [10][17][10][19]		
Salt	Melting point [°C]	Max working temperature [°C]
FLiBe	459.9	> 1400
FLiNaK	453.9	> 1400
NaCl-KCl- MgCl <sub>2</sub>	385	800
LiCl-KCl	355	1400

### 4. Results and Conclusions

In this study, the optimization of the superheated steam Rankine cycle, under the given outlet conditions of the molten salt reactor's steam generator, showed that when efficiency exceeds 40%, the steam generator inlet temperature reaches 284.9 °C. The corresponding Temperature-Entropy (T-S) diagram for this case is shown in Figure 5.

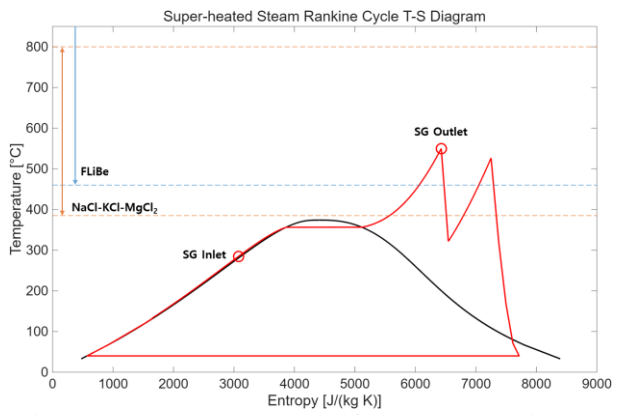


Fig 5. Superheated Steam Rankine Cycle T-S Diagram

When the maximum steam generator inlet temperature was compared with the melting points of candidate salts, it was found to be approximately 184 °C lower than the melting point of FLiBe and about 100 °C lower than that of NaCl-KCl-MgCl2. In other words, even with the steam Rankine cycle—the superheated technologically mature option currently available—the possibility of salt freezing in this region cannot be eliminated. While these findings are derived from a cycle-level analysis, a more precise evaluation of freezing potential would require additional studies on steam generator design and solidification behavior. Nevertheless, the present results confirm that salt solidification may occur on the outer surface of the steam generator tubes, highlighting the necessity of further analysis and design measures to address this issue.

## ACKNOWLEDGEMENT

This work was supported by the Nuclear Safety Research Program through the Korea Foundation Of Nuclear Safety (KoFONS) using the financial resource granted by the Nuclear Safety and Security Commission (NSSC) of the Republic of Korea. (No. RS-2023-00244146)

#### REFERENCES

[1] Zheng, C., Cheng, K., & Han, D. (2025). High-Temperature Molten Salt Heat Exchanger Technology: Research Advances, Challenges, and Future Perspectives. Energies, 18(12), 3195. https://doi.org/10.3390/en18123195

[2] Kartal, M.A. (2025). Investigation and Energy Modeling of New Generation Environmentally Friendly Energy Source Thorium Fueled Molten Salt Reactors. Igmin Research. https://www.igminresearch.jp/articles/html/igmin300

[3] Şahin, H.M., Şahin, S., Tunc, G., & Sahiner, H. (2025). Neutronic Study of ThF<sub>4</sub>-UF<sub>4</sub>-LiF Fuel Mixture

in the Molten Salt Hybrid Reactor for <sup>233</sup>U Denaturing. SSRN.

https://papers.ssrn.com/sol3/papers.cfm?abstract\_id=52 93739

[4] Mehos, M., Turchi, C., Vidal, J., Wagner, M., Ma, Z., & Ho, C. (2017). Concentrating Solar Power Gen3 Demonstration Roadmap. U.S. Department of Energy, Office of Scientific and Technical Information. https://www.osti.gov/servlets/purl/1338899

[5] Sabharwall, P., et al. (2013). Molten Salt Reactors — System and Technology Overview. Nuclear Technology, 180(1), 16–31. https://doi.org/10.13182/NT13-A13674

[6] International Atomic Energy Agency. (2021). Advances in Small Modular Reactor Technology Developments. IAEA-TECDOC-1930.

https://www.iaea.org/publications/14778

[7] Kehlhofer, R., Warner, J., Nielsen, P., & Bachmann, R. (2009). Combined-Cycle Gas & Steam Turbine Power Plants (3rd ed.). PennWell Books.

[8] Chao, R., et al. (2016). Thermodynamic Optimization of Regenerative Feedwater Heating Systems in Steam Power Plants. Energy Conversion and Management, 111, 391–401.

https://doi.org/10.1016/j.enconman.2015.12.065

[9] Williams, D. F., Del Cul, G. D., & Toth, L. M. (2006). Assessment of Candidate Molten Salt Coolants for the NGNP/NHI Heat-Transfer Loop. Oak Ridge National Laboratory, ORNL/TM-2006/69.

https://info.ornl.gov/sites/publications/files/Pub61018.p df

[10] Ignatiev, V. V., et al. (2019). Molten Salts for Nuclear Reactors and Energy Storage: State of the Art. Journal of Nuclear Materials, 517, 371–383. https://doi.org/10.1016/j.jnucmat.2019.02.037

[11] Ambrosek, J. W., et al. (2009). Thermophysical Properties for Molten Salts Used in Nuclear Systems. Idaho National Laboratory, INL/EXT-09-16506. https://inldigitallibrary.inl.gov/sites/sti/4500043.pdf [12] Bradshaw, R. W., & Siegel, N. P. (2008). Molten

[12] Bradshaw, R. W., & Siegel, N. P. (2008). Molten nitrate salt development for thermal energy storage in parabolic trough solar power systems. Journal of Solar Energy Engineering, 130(4), 041007.

[13] Summers, K., & Chidambaram, D. (2021). Corrosion in molten salts for solar thermal power. The Electrochemical Society Interface, 30(2), 71–76.

[14] Carotti, M., Venneri, F., & Merle-Lucotte, E. (2020). Tritium generation and transport in molten salt reactors: A review. Annals of Nuclear Energy, 140, 107228.

[15] LeBlanc, D. (2010). Molten salt reactors: A new beginning for an old idea. Nuclear Engineering and Design, 240(6), 1644–1656.

[16] Sonia Fereres, Cristina Prieto, Pau Giménez-Gavarrell, Alfonso Rodríguez, Pedro Enrique Sánchez-Jiménez, Luis A. Pérez-Maqueda, Molten carbonate salts for advanced solar thermal energy power plants: Cover gas effect on fluid thermal stability, Solar Energy Materials and Solar Cells, Volume 188, 2018, Pages 119-126, ISSN 0927-0248

- [17] Li, Peiwen & Molina, Edgar & Wang, Kai & Xu, Xiankun & Dehghani, Ghazal & Kohli, Amit & Hao, Qing & Kassaee, Mohamad & Jeter, Sheldon & Teja, Amyn. (2016). Thermal and Transport Properties of NaCl-KCl-ZnCl2 Eutectic Salts for New Generation High Temperature Heat Transfer Fluids. Journal of Solar Energy Engineering. 138. 10.1115/1.4033793.
- [18] Carolina Villada, Wenjin Ding, Alexander Bonk, Thomas Bauer, Engineering molten MgCl2–KCl–NaCl salt for high-temperature thermal energy storage: Review on salt properties and corrosion control strategies, Solar Energy Materials and Solar Cells, Volume 232, 2021, 111344, ISSN 0927-0248
- [19] Sohal, Manohar & Ebner, Matthias & Sabharwall, Piyush & Sharpe, Phil. (2010). Engineering Database of Liquid Salt Thermophysical and Thermochemical Properties. Idaho Natl. Lab. Idaho Falls CrossRef. 10.2172/980801